



Effects of Electrode-Tissue Proximity on Cardiac Lesion Formation Using Pulsed Field Ablation

Brian Howard, PhD; Atul Verma¹, MD; Wendy S. Tzou², MD; Lars Mattison, PhD; Bor Kos³, PhD; Damijan Miklavčič⁴, PhD; Birce Onal⁵, PhD; Mark T. Stewart⁶, BS; Daniel C. Sigg⁷, MD, PhD

BACKGROUND: Pulsed field ablation (PFA) is a novel energy modality for treatment of cardiac arrhythmias. The impact of electrode-tissue proximity on lesion formation by PFA has not been conclusively assessed. The objective of this investigation was to evaluate the effects of electrode-tissue proximity on cardiac lesion formation with a biphasic, bipolar PFA system.

METHODS: PFA was delivered on the ventricular epicardial surface in an isolated porcine heart model (n=8) via a 4-electrode prototype catheter. An offset tool was designed to control the distance between electrodes and target tissue; deliveries were placed 0 mm (0 mm offset), 2 mm (2 mm offset), and 4 mm away from the tissue (4 mm offset). Lesions were assessed using tetrazolium chloride staining. Numerical models for the experimental setup with and without the offset tool validated and supported results.

RESULTS: Cardiac lesion dimensions decreased proportional to the distance between epicardial surface and electrodes. Lesion depth averaged 4.3 ± 0.4 mm, 2.7 ± 0.4 mm, and 1.3 ± 0.4 mm for the 0, 2, and 4 mm and lesion width averaged 9.4 ± 1.1 mm, 7.5 ± 0.8 mm and 5.8 ± 1.4 mm for the 0, 2, and 4 mm offset distances, respectively. Numerical modeling matched ex vivo results well and predicted lesion creation with and without the offset tool.

CONCLUSIONS: Using a biphasic, bipolar PFA system resulted in cardiac lesions even in the 0 mm offset distance case. The relationship between lesion depth and offset distance was linear, and the deepest lesions were created with 0 mm offset distance, that is, with electrodes in contact with tissue. Therefore, close electrode-tissue proximity increases the likelihood of achieving transmural lesions by maximizing the electric field penetration into the target tissue.

GRAPHIC ABSTRACT: A graphic abstract is available for this article.

Key Words: arrhythmia, cardiac ■ atrial fibrillation ■ cardiac ablation ■ chloride ■ electrode

Thermal-based catheter ablation systems (eg, radiofrequency and cryoablation) are the cornerstone treatment modalities for patients with antiarrhythmic drug resistant, symptomatic paroxysmal, and persistent atrial fibrillation.¹ Standard catheter ablation technologies depend upon electrode-tissue contact to optimize lesion delivery and clinical outcomes.^{2,3} Lack of contact with the tissue during ablation may lead to ineffective lesion formation using thermal technologies, although an important balance is often necessary to prioritize safety

and avoid excessive energy delivery. Therefore, operators rely on multiple surrogate indicators of stable and safe catheter-tissue placement including the additional use of tactile feedback, contact force measurements, impedance and electrode temperature measurements, and identification of catheter location by imaging.⁴⁻⁷

Pulsed field ablation (PFA) is an emerging energy modality for catheter-based treatment of cardiac arrhythmias currently in clinical development.⁸⁻¹¹ PFA employs a nonthermal ablative mechanism of action called

Correspondence to: Daniel C. Sigg, MD, PhD, Medtronic - MVS46, 8200 Coral Sea St NE, Mounds View, MN 55112. Email daniel.c.sigg@medtronic.com

This article was sent to N.A. Mark Estes III, MD, Guest Editor, for review by expert referees, editorial decision, and final disposition.

Supplemental Material is available at <https://www.ahajournals.org/doi/suppl/10.1161/CIRCEP.122.011110>.

For Sources of Funding and Disclosures, see page 712.

© 2022 The Authors. *Circulation: Arrhythmia and Electrophysiology* is published on behalf of the American Heart Association, Inc., by Wolters Kluwer Health, Inc. This is an open access article under the terms of the [Creative Commons Attribution Non-Commercial-NoDerivs](https://creativecommons.org/licenses/by-nc-nd/4.0/) License, which permits use, distribution, and reproduction in any medium, provided that the original work is properly cited, the use is noncommercial, and no modifications or adaptations are made.

Circulation: Arrhythmia and Electrophysiology is available at www.ahajournals.org/journal/circep

WHAT IS KNOWN?

- Temperature-based ablation technologies such as radiofrequency ablation or cryoablation require direct tissue contact for energy transfer.
- Pulsed field ablation is a field-based technology resulting in cell death via exposure of tissue to electric fields exceeding the threshold for irreversible electroporation.

WHAT THIS STUDY ADDS

- Although ablation using pulsed fields does not require direct tissue contact for myocardial lesion creation, the deepest lesion were observed with direct tissue contact.

Nonstandard Abbreviations and Acronyms

| | |
|------------|-----------------------|
| PFA | pulsed field ablation |
| TTC | tetrazolium chloride |

irreversible electroporation, in which application of high voltage electric pulses induces transient permeabilization of cell membranes which (subsequently) leads to cell death.^{12–15} This mechanism is linked with potential clinical benefits, including avoiding/reducing the probability of forming atrioesophageal fistula and reduction in pulmonary vein stenosis.¹⁶ Additionally, existing preclinical work indicated that the heavily trabeculated appendages can be ablated in a durable, transmural manner with a circular PFA catheter.¹⁷ Nevertheless, the impact of electrode-tissue proximity on cardiac lesion formation with a biphasic, bipolar PFA system has not been conclusively assessed.

In our study, we hypothesize that direct electrode-tissue contact is not required to create effective cardiac lesions with PFA, due to irreversible electroporation dependence on the electric field distribution. We aimed to identify the impact of electrode-tissue proximity on lesion creation in an isolated porcine heart model using a prototype catheter and replicated these results with numerical modeling.

METHODS

This research protocol was approved by the Institutional Animal Care and Use Committee of the University of Minnesota and the animal experiments were performed at the University of Minnesota. The data that support the findings of this study are available from the corresponding author upon reasonable request.

Isolated Heart Preparation

Isolated hearts were prepared from male Yorkshire pigs ($n=8$, mean weight 76.4 ± 9.4 kg [SD]) as previously described.¹⁸ In

brief, the hearts are explanted in toto, and, after a period of cardioplegic cardiac arrest, reperfused with modified Krebs-Henseleit buffer during which sinus cardiac rhythm, physiological temperatures (37°C), and pressures were maintained throughout the experiment.

Overview of Experimental Procedure

The isolated porcine heart was reanimated on the apparatus,¹⁸ and once stable function was achieved, lesions were created on the epicardial surface of the beating ventricles using an offset tool filled with heparinized blood, PFA catheter, and PFA generator as described below. Three to 5 PFA lesions were created on the epicardial surface of the heart. For each lesion, 4 pulse trains were delivered. The left ventricle was chosen due to its wall thickness, to optimize a lesion dose-response curve. After a period of 2 hours of continued beating heart perfusion, tissue sections were excised for imaging. Freshly excised lesions, the triphenyl tetrazolium chloride (TTC) stained lesions, and cross-sections of TTC-stained lesions were imaged and analyzed using ImageJ software.¹⁹ Cross-sectioning was performed on the long axis of the lesion approximately orthogonal to the surface.

PFA Catheter and System

A prototype PFA catheter with a linear arrangement of 4 electrodes was built as shown in Figures 1A and 1B. A custom PFA research generator delivered 4 trains of high-voltage (1500 V) biphasic, bipolar pulses to the catheter.

Offset Tool

An offset tool was developed to precisely control distance of the PFA electrodes from the epicardial surface (Figure 1A through 1C). Using different configurations, this tool allowed the PFA electrode array to be placed either directly on the epicardial surface (0 mm, Figure 1D, left), or at an offset of either 2 mm or 4 mm (Figure 1D, middle and right, respectively) as measured between the electrodes and the tissue surface. The electrodes were held against the pegs opposite of the tissue to ensure that there were no obstructions between the electrode array and the tissue to minimize any effect of the tool on the electric field distribution. During energy delivery, the catheter electrode chamber of the offset tool was filled with noncirculating heparinized blood. Three to 5 lesions were made on each porcine heart. Each heart had ablations performed at 0, 2, and 4 mm offset with additional ablations randomized (giving equal probability to additional 0, 2, and 4 mm offset) when surface area allowed.

Lesion Imaging and Analysis

The primary endpoint to demonstrate the effect of electrode-tissue proximity on PFA ablation was lesion depth. Tissue was stained using 1% TTC at $\approx 37^\circ\text{C}$ for 3 minutes. Lesion dimensions were then measured using ImageJ software (National Institute of Health).

Modeling

COMSOL Multiphysics (Comsol AB, Stockholm, Sweden) was used for numerical simulation. The CAD model of the offset

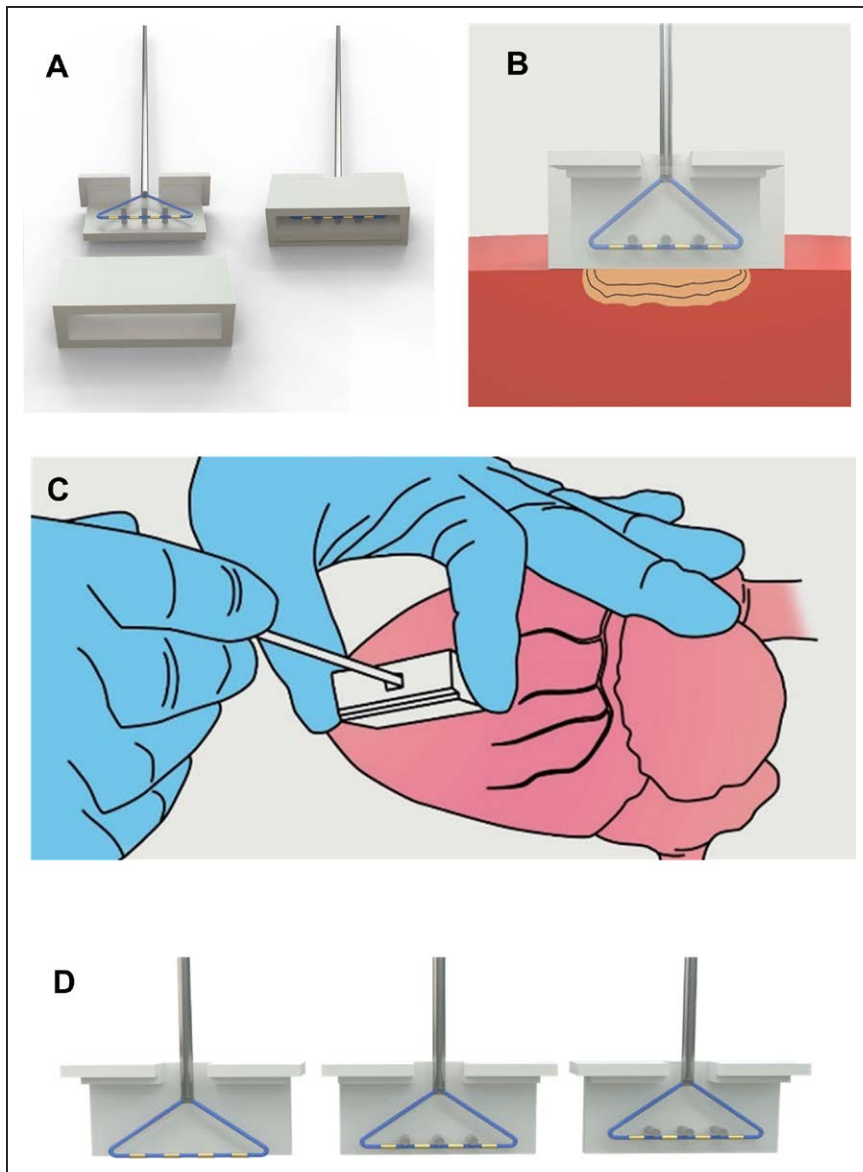


Figure 1. Offset tool and experimental setup.

Pulsed field ablation (PFA) catheter with linear 4-electrode array with offset tool open and electrode 1 on the far left (**A**). The catheter located within the offset tool (with transparent front view) as well as a rendering of the cardiac pulsed field ablation lesion is shown (**B**). Experimental setup during epicardial PFA lesion creation. The chamber was filled with heparinized blood prior to initiating pulsed field ablation deliveries. **C**, During placement of the offset apparatus with electrode array positioned against epicardial surface, there was direct electrode-tissue proximity (0 mm, **left**) or the catheter was pulled back against the pins to ensure consistent distance from the tissue for 2 mm (**middle**) and 4 mm (**right**) electrode-tissue distances (**D**).

tool and catheter was placed adjacent to a 35×65×10 mm cuboid representing the ventricular tissue. A cuboid with the same dimensions was placed below the ventricular tissue to represent the perfusate-filled heart chamber (Figure 2). The

tissue was modeled with anisotropic conductivity of myocardium, with a change in fiber direction of 180° between the epicardial and endocardial surface.²⁰ The tissue conductivity also included an electric field-dependent conductivity increase.

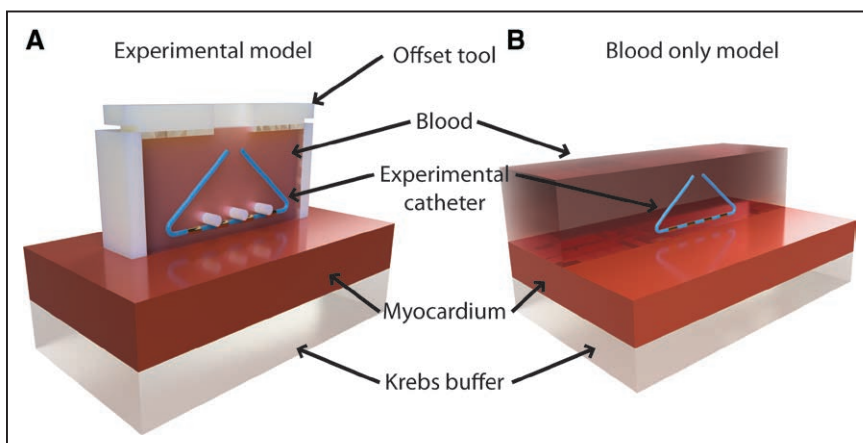


Figure 2. Visual comparison of the 2 COMSOL Multiphysics geometries used in the numerical simulations at a distance of 2 mm from tissue.

Both parts have the blood (and offset tool) cut out for better clarity through a plane passing through the center of the experimental catheter. **A**, Numerical model. **B**, Numerical model without offset tool. The blood pool and myocardium were extended by 10 mm on each side to prevent the edge of the model space from affecting the results.

A similar model was created (marked as unlimited model) in which the offset tool was removed (Figure 2). A more detailed description of the model and equations used in the modeling as well as the material properties used in the simulations are listed in [Supplementary Materials \(Table S1\)](#).

The models were solved in a time domain study, where 1500 V was applied to the electrodes as a boundary condition. The calculated electric field at the end of the pulse trains was exported to MATLAB (Mathworks, Natick, MA) for extracting the lesion width and depth in the same locations as in the experiments. For model validation, simulated current was compared with measured values, and a good agreement was obtained (Table S2).

The numerical model was used to extract lesion depths at 7 sites below the catheter using a range of electric field thresholds (400–800 V/cm in 10 V/cm increments). These data were used to train an explicit numerical model of depth as a function of electrode-tissue distance and threshold that included all values not directly modeled. Subsequently, this model was used to calculate the threshold electric field value for the cardiac tissue that best fit each experimental result.

Statistical Methods

One-way ANOVA using the Tukey method for multiple comparisons or linear regression analyses was used to evaluate the relationship between lesion size and offset of lesions (Minitab 20.1.3). A mixed effects model was used to evaluate inter-animal variability. Statistical significance was inferred if *P* values were <0.05.

RESULTS

Lesion Assessment (Isolated Heart Tissue)

A total of 32 ablations were performed across the 8 hearts; 11 at 0 mm offset, 11 at 2 mm offset, and 10

at 4 mm offset. Figure 3 shows superficial TTC-stained images from transversely cut tissue (left) and uncut tissue slices (right) for PFA applications at 0 mm, 2 mm and 4 mm offset. Lesion depth (Figure 4A and 4B) and width (Figure 4C and 4D) decreased significantly as the distance between epicardial surface and electrodes increased. Lesion depths averaged 4.3 ± 0.4 mm, 2.7 ± 0.4 mm, and 1.3 ± 0.4 mm for the 0, 2, and 4 mm electrode-tissue distances, respectively. Lesion widths averaged 9.4 ± 1.1 mm, 7.5 ± 0.8 mm, and 5.8 ± 1.4 mm for the 0, 2, and 4 mm electrode-tissue distances, respectively. Shown are individual lesion depths (in mm) with linear regression curves (Figure 4A: linear slope -0.7413 , $R^2=0.91$, $P<0.0001$; Figure 4C: linear slope -0.8979 , $R^2=0.65$, $P<0.0001$), as well as Box-Whiskers plots with median, 25th to 75th percentile and minimum to maximum whiskers (Figure 4B and 4D). One-way ANOVA analysis using the Tukey multiple comparison test showed significant differences between the 0 mm, 2 mm, and 4 mm groups (*P* values for between-group comparisons are $P<0.001$ for depth, and $P<0.01$ for width). Accounting for multiple lesions performed on each porcine heart with a mixed model, the results were similar to the linear regression model due to no significant difference or major variability in lesion depth or width between each animal.

Numerical Modeling

The average lethal dose threshold value of cardiac tissue ($N=6$) was determined to be 489 ± 22 V/cm. That means the model on average best matched the ex vivo data when 489 ± 22 V/cm was used as the threshold for defining the lesion boundary. This value was used to

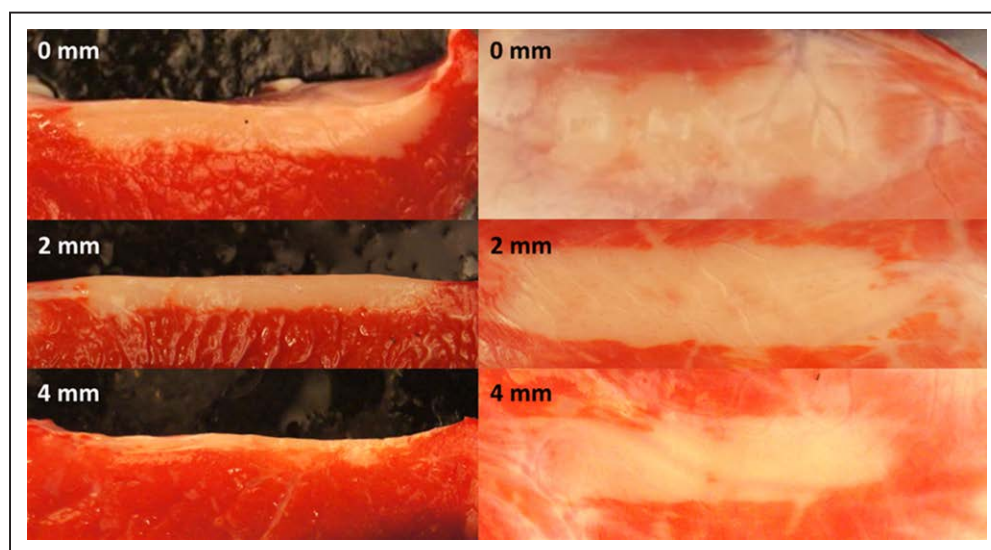


Figure 3. Sample lesion images.

We need to change this Figure legend to as follows: Shown are superficial tetrazolium chloride (TTC) stained images from transversely cut tissue slices (**left**) at 0 mm, 2 mm, and 4 mm offset as well as uncut tissue slices (lesions seen from above, width measurements indicated by yellow lines, **right**).

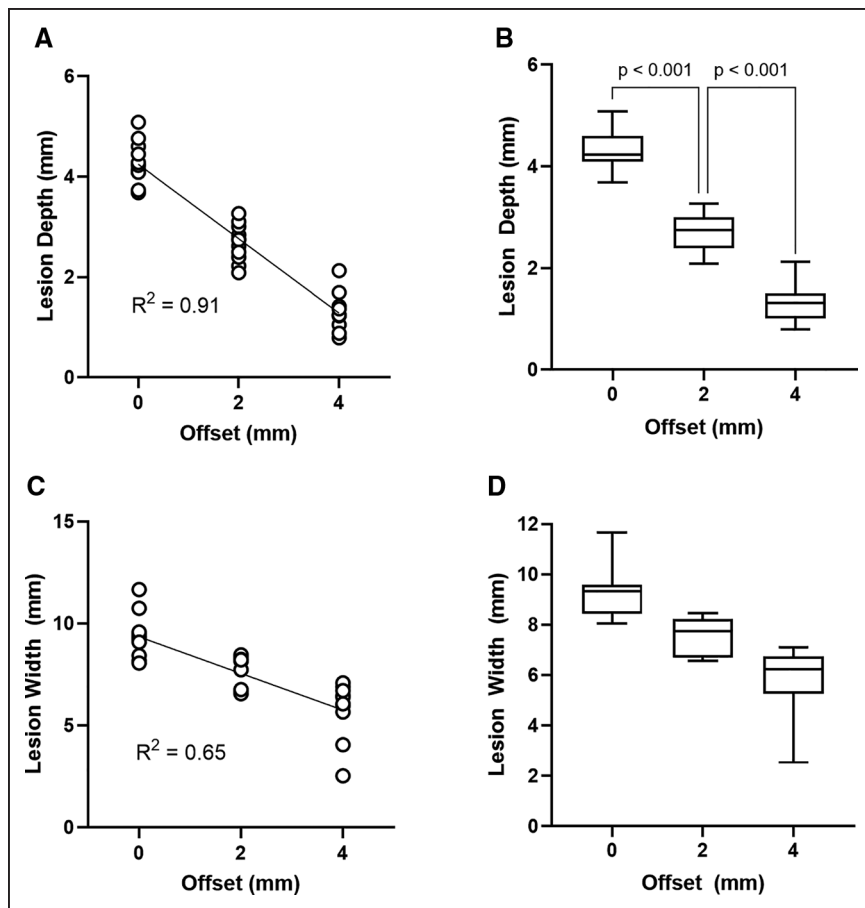


Figure 4. Lesion depth (A and B) and width (C and D) decreased significantly as the distance between epicardial surface and electrodes increased.

Shown are individual lesion depths (in mm) with linear regression curves (**A**: linear slope -0.7413 , $R^2=0.91$; **C**: linear slope -0.8979 , $R^2=0.65$) as well as Box-Whiskers plots with median, 25th to 75th percentile and minimum to maximum whiskers (**B** and **D**). Lesion depth-averaged 4.3 ± 0.4 mm, 2.7 ± 0.4 mm, and 1.3 ± 0.4 mm for the 0-, 2-, and 4-mm electrode-tissue distances respectively. Lesion width averaged 9.4 ± 1.1 mm, 7.5 ± 0.8 mm, and 5.8 ± 1.4 mm for the 0-, 2-, and 4-mm electrode-tissue distances respectively. One-way ANOVA analysis using the Tukey multiple comparison test showed significant differences between the 0 mm, 2 mm, and 4 mm groups ($P < 0.001$ for depth, and $P < 0.01$ for width).

generate 2 optimized models: the Numerical model and the Numerical model without the offset tool (Figure 5).

Figure 6 presents the ex vivo data, the modeling of the ex vivo data (Numerical model), and an infinite blood pool model which removes the offset tool (Numerical model without the offset tool). The results of the numerical models correspond well with linear trends observed in the ex vivo data. Regression lines calculated for the ex vivo data and the Numerical model had slopes of -0.740 and -0.723 (mm depth/mm offset) respectively (regression lines are not shown in Figure 6). The Numerical model without the offset tool had a slope of -0.947 (mm depth/mm offset).

DISCUSSION

We have demonstrated that biphasic, bipolar PFA delivers using a prototype catheter can form cardiac lesions even in the absence of direct electrode-tissue contact. Although direct electrode-tissue contact was not required to achieve a lesion, we demonstrated that a distance of 0 mm between the electrodes and target tissue resulted in the deepest lesions. The relationship between electrode-tissue proximity and lesion size showed a high linear correlation of $R^2=0.91$. Furthermore, comparison of the experimental results to numerical modeling gave an estimate of the threshold value of cardiac susceptibility

to PFA of 489 ± 22 V/cm, which needs to be considered specific to this waveform delivery and system.

Existing preclinical work has indicated that heavily trabeculated appendages can be ablated in a durable, transmural manner with a circular PFA catheter, providing indirect evidence that PFA may result in lesions without direct electrode-tissue contact.¹⁶ Recently, Nakagawa et al²¹ reported no lesions when a focal catheter (3.5 mm irrigated TactiCath SE, Abbott) was ≈ 2 mm from the endocardium after PFA (Centauri, Galaxy Medical) when used in conjunction with electro-anatomical mapping and a unipolar PFA ablation system. Nevertheless, the well-controlled electrode-tissue proximity used in our study provides direct evidence of the ability of a biphasic, bipolar PFA system to create cardiac lesions in a beating heart ex vivo in the 0 mm offset distance case. Given challenges in achieving consistent and safe catheter stability using standard ablation catheters, particularly in trabeculated tissue or intracavitary cardiac structures, the ability to create lesions without need for perfect placement of electrodes on the target tissue is appealing.

Lesion dimension assessments were consistent with numerical modeling; both lesion depth and width decrease with increasing electrode-tissue distance. The slopes observed in the ex vivo study and the numerical model showed values of -0.74 (ex vivo), and -0.72 (Numerical model), respectively. This means that for every millimeter

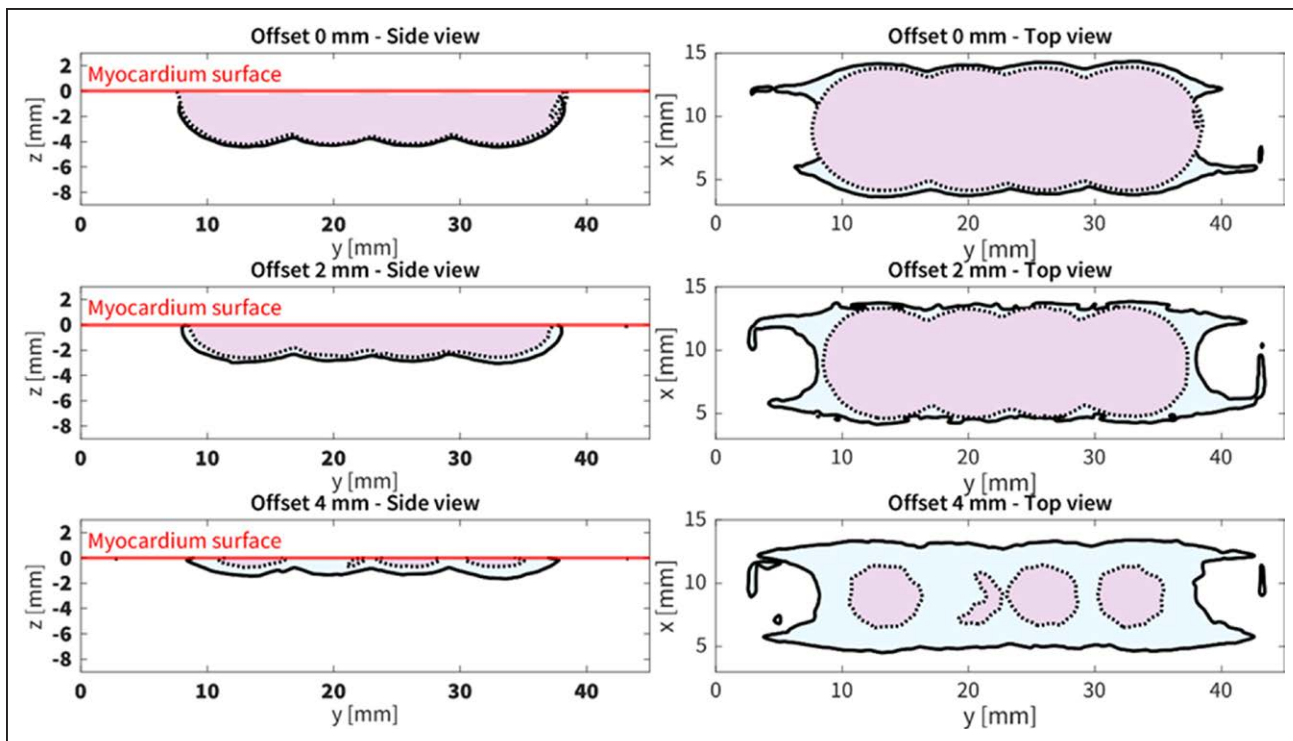


Figure 5. Numerically predicted lesion sizes.

This figure shows the Numerical model (blue area, continuous outline) compared with the Numerical model without the offset tool (pink area, dotted outline). The offset tool induced some additional lesion formation at the edges, where the concentration of the current density resulted in higher local electric field in comparison to the unlimited model, which is most obvious in the top view and consistent with the experimental results shown in Figure 2.

of offset distance added, the lesion depth decreased by an average of 0.74 mm (*ex vivo*) and 0.72 mm (Numerical model). However, when modeling the system without the offset tool (Numerical model without the offset tool), the calculated slope was -0.945 , suggesting that the field distribution in blood and tissue was similar and approximating a 1:1 relationship.

Although these findings are specific to this device and waveform, clinically these results may be relevant to the growing field of PFA, in which multiple systems are employing multipolar PFA catheters.

This is advantageous since larger regions can be targeted (like entire pulmonary veins), allowing for a shorter, more time-efficient procedure. However, given the natural variations in human cardiac anatomy, it is often not possible to orient a large, multipolar device to have complete and perfect electrode-tissue proximity along its entire circumference. As we are still able to create lesions without direct electrode-tissue contact, PFA can be considered more forgiving than thermal sources of ablation where a lack of direct electrode-tissue proximity results in no lesion

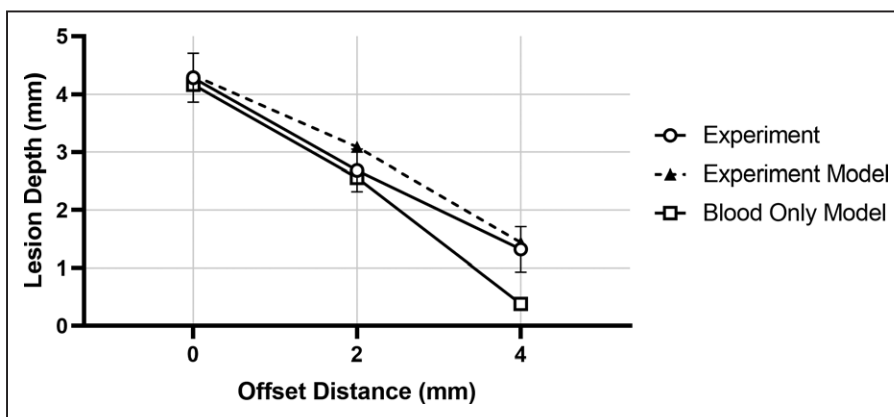


Figure 6. Lesion depth as a function of offset distance observed experimentally (*ex vivo*), compared to lesion depth calculated using a numerical model mimicking the experimental model (numerical model), as well as using a model in which the offset tool was removed (numerical model without offset tool).

Downloaded from <http://ahajournals.org> by on October 18, 2022

formation. However, inadequate lesion formation may result without direct electrode-tissue contact.²² Current clinical workflow of most PFA systems involving multiple applications and overlapping catheter positioning is therefore likely justified to ensure optimal, contiguous lesion formation.

Limitations

This experimental study was conducted under controlled laboratory conditions using an isolated porcine working heart model perfused with Krebs-Henseleit buffer. Only the ventricular myocardium was targeted in order to facilitate clear lesion visualization and measurements. Applicability of this work to clinical practice will require further study, including in diseased cardiac tissues (eg, remodeled atrial tissue, infarcted fibrotic ventricular tissue) and long-term durability of lesions. With regards to the limitation of lesion durability, it should be noted that tetrazolium chloride has been shown to correlate very well with histological cell damage in cardiac ischemic cell death and is widely used in preclinical histopathological studies.²³ Also, reported lesion dimensions of these epicardial lesions may not be representative of endocardial lesion dimensions.

In order to address the potential limitation of directing the electrical field with the offset tool, we modeled the catheter offset and its effects on cardiac lesions without the offset tool. The Unlimited model was comprehensive, including electrical and thermal conductivity and heat capacity (Supplementary Appendix). Although a small effect of the offset tool was observed, the numerical model with the offset tool matched the experimental setup very well, providing good confidence that the Unlimited model represents reality accurately.

This investigation employed a prototype catheter that was custom-built for research purposes and does not represent PFA systems in clinical use. Each PFA system design is different, and this data cannot be extrapolated to other PFA systems, waveforms, or catheters. Furthermore, we have only investigated one set of pulse wave parameters based on what has been investigated in the PULSED AF clinical study (<https://clinicaltrials.gov/ct2/show/NCT04198701>), which has not yet been Food and Drug Administration approved or received regulatory approval for commercialization.¹¹ For example, we do not know if a similar phenomenon could be observed using unipolar PFA delivery.

Conclusions

This study provides strong evidence that pulsed electric fields create cardiac lesions even in the absence of direct electrode-tissue contact case. We demonstrate lesion creation even when the PFA electrodes were as far as

4 mm from the epicardial surface. However, the optimal, deepest lesions were created with 0 mm offset distance.

ARTICLE INFORMATION

Received March 30, 2022; accepted September 12, 2022.

Affiliations

Medtronic, Minneapolis, MN (B.H., L.M., B.O., M.T.S., D.C.S.). McGill University Health Center, McGill University, Montreal, Quebec, Canada (A.V.). University of Colorado School of Medicine, Aurora, CO (W.S.T.). University of Ljubljana, Slovenia (B.K., D.M.).

Sources of Funding

This study was funded by Medtronic.

Disclosures

Dr Howard, Dr Mattison, Dr Onal, M.T. Stewart, and Dr Sigg are employees of Medtronic. Drs Verma, Tzou, Kos, and Miklavčič are Medtronic consultants.

Supplemental Material

Supplemental Methods
Detailed Model Description
Tables S1–S2
References^{24–29}

REFERENCES

- Calkins H, Hindricks G, Cappato R, Kim Y, Saad EB, Aguinaga L, Akar JG, Badhwar V, Brugada J, Camm J et al. 2017 HRS/EHRA/ECAS/APHS/SOLAECE expert consensus statement on catheter and surgical ablation of atrial fibrillation. *Heart Rhythm*. 2017;14:e275–e444. doi: 10.1016/j.hrthm.2017.05.012
- Natale A, Reddy VY, Monir G, Wilber DJ, Lindsay BD, McElderry HT, Kantipudi C, Mansour MC, Melby DP, Packer DL et al. Paroxysmal AF catheter ablation with a contact force sensing catheter: results of the prospective, multicenter SMART-AF trial. *J Am Coll Cardiol*. 2014;64:647–656. doi: 10.1016/j.jacc.2014.04.072
- Reddy VY, Shah D, Kautzner J, Schmidt B, Saoudi N, Herrera C, Jais P, Hindricks G, Peichl P, Yulzari A et al. The relationship between contact force and clinical outcome during radiofrequency catheter ablation of atrial fibrillation in the TOCCATA study. *Heart Rhythm*. 2012;9:1789–1795. doi: 10.1016/j.hrthm.2012.07.016
- Ullah W, Hunter RJ, Haldar S, McLean A, Dhinoja M, Sporton S, Earley MJ, Lorgat F, Wong T, Schilling RJ. Comparison of robotic and manual persistent AF ablation using catheter contact force sensing: an international multicenter registry study. *Pacing Clin Electrophysiol*. 2014;37:1427–1435. doi: 10.1111/pace.12501
- Shurrab M, Di Biase L, Briceno DF, Kaoutskia A, Haj-Yahia S, Newman D, Lashevsky I, Nakagawa H, Crystal E. Impact of contact force technology on atrial fibrillation ablation: a meta-Analysis. *J Am Heart Assoc*. 2015;4:e002476. doi: 10.1161/JAHA.115.002476
- Rozen G, Ptaszek L, Zilberman I, Cordaro K, Heist EK, Beeckler C, Altmann A, Ying Z, Liu Z, Ruskin JN et al. Prediction of radiofrequency ablation lesion formation using a novel temperature sensing technology incorporated in a force sensing catheter. *Heart Rhythm*. 2017;14:248–254. doi: 10.1016/j.hrthm.2016.11.013
- Haines DE. The biophysics of radiofrequency catheter ablation in the heart: the importance of temperature monitoring. *Pacing Clin Electrophysiol*. 1993;16:586–591. doi: 10.1111/j.1540-8159.1993.tb01630.x
- Reddy VY, Anter E, Rackauskas G, Peichl P, Koruth JS, Petru J, Funasako M, Minami K, Natale A, Jais P et al. Lattice-tip focal ablation catheter that toggles between radiofrequency and pulsed field energy to treat atrial fibrillation: a first-in-human trial. *Circ Arrhythm Electrophysiol*. 2020;13:e008718. doi: 10.1161/CIRCEP.120.008718
- Reddy VY, Neuzil P, Koruth JS, Petru J, Funasako M, Cochet H, Sediva L, Chovanec M, Dukkkipati SR, Jais P. Pulsed field ablation for pulmonary vein isolation in atrial fibrillation. *J Am Coll Cardiol*. 2019;74:315–326. doi: 10.1016/j.jacc.2019.04.021
- Loh P, van Es R, Groen MHA, Neven K, Kassenberg W, Wittkamp FHM, Doevendans PA. Pulmonary vein isolation with single pulse

- irreversible electroporation: a first in human study in 10 patients with atrial fibrillation. *Circ Arrhythm Electrophysiol.* 2020;13:e008192. doi: 10.1161/CIRCEP.119.008192
11. Verma A, Boersma L, Haines DE, Natale A, Marchlinski FE, Sanders P, Calkins H, Packer DL, Hummel J, Onal B, et al. First-in-human experience and acute procedural outcomes using a novel pulsed field ablation system: the PULSED AF pilot trial. *Circ Arrhythm Electrophysiol.* 2021;Circcep.121010168. doi: 10.1161/circep.121.010168
 12. Kotnik T, Rems L, Tarek M, Miklavcic D. Membrane electroporation and electroporabilization: mechanisms and models. *Annu Rev Biophys.* 2019;48:63–91. doi: 10.1146/annurev-biophys-052118-115451
 13. Neumann E, Kakorin S. Membrane electroporation: chemical thermodynamics and flux kinetics revisited and refined. *Eur Biophys J.* 2018;47:373–387. doi: 10.1007/s00249-018-1305-3
 14. Garcia PA, Davalos RV, Miklavcic D. A numerical investigation of the electric and thermal cell kill distributions in electroporation-based therapies in tissue. *PLoS One.* 2014;9:e103083. doi: 10.1371/journal.pone.0103083
 15. Batista Napotnik T, Polajžer T, Miklavčič D. Cell death due to electroporation - a review. *Bioelectrochemistry.* 2021;141:107871. doi: 10.1016/j.bioelechem.2021.107871
 16. Howard B, Haines DE, Verma A, Packer D, Kirchhof N, Barka N, Onal B, Fraasch S, Miklavčič D, Stewart MT. Reduction in pulmonary vein stenosis and collateral damage with pulsed field ablation compared with radiofrequency ablation in a canine model. *Circ Arrhythm Electrophysiol.* 2020;13:e008337. doi: 10.1161/CIRCEP.120.008337
 17. Stewart MT, Haines DE, Miklavčič D, Kos B, Kirchhof N, Barka N, Mattison L, Martien M, Onal B, Howard B, et al. Safety and chronic lesion characterization of pulsed field ablation in a Porcine model. *J Cardiovasc Electrophysiol.* 2021;32:958–969. doi: 10.1111/jce.14980
 18. Chinchoy E, Soule CL, Houlton AJ, Gallagher WJ, Hjelle MA, Laske TG, Morissette J, Iazzo PA. Isolated four-chamber working swine heart model. *Ann Thorac Surg.* 2000;70:1607–1614. doi: 10.1016/s0003-4975(00)01977-9
 19. Schneider CA, Rasband WS, Eliceiri KW. NIH image to imageJ: 25 years of image analysis. *Nat Methods.* 2012;9:671–675. doi: 10.1038/nmeth.2089
 20. Xie F, Zemlin CW. Effect of twisted fiber anisotropy in cardiac tissue on ablation with pulsed electric fields. *PLoS One.* 2016;11:e0152262. doi: 10.1371/journal.pone.0152262
 21. Nakagawa H, Castellvi Q, Neal R, Girouard S, Ikeda A, Kuroda S, Hussein AA, Saliba WJ, Wazni OM. B-PO03-131 effects of contact force on lesion size during pulsed field ablation. *Heart Rhythm.* 2021;18:S242–S243.
 22. Hocini M, Condie C, Stewart MT, Kirchhof N, Foell JD. Predictability of lesion durability for AF ablation using phased radiofrequency: power, temperature, and duration impact creation of transmural lesions. *Heart Rhythm.* 2016;13:1521–1526. doi: 10.1016/j.hrthm.2016.02.012
 23. Fishbein MC, Meerbaum S, Rit J, Lando U, Kanmatsuse K, Mercier JC, Corday E, Ganz W. Early phase acute myocardial infarct size quantification: validation of the triphenyl tetrazolium chloride tissue enzyme staining technique. *Am Heart J.* 1981;101:593–600. doi: 10.1016/0002-8703(81)90226-x
 24. Steendijk P, van der Velde ET, Baan J. Dependence of anisotropic myocardial electrical resistivity on cardiac phase and excitation frequency. *Basic Res Cardiol.* 1994;89:411–426. doi: 10.1007/BF00788279
 25. Vetter FJ, Simons SB, Mironov S, Hyatt CJ, Pertsov AM. Epicardial fiber organization in swine right ventricle and its impact on propagation. *Circ Res.* 2005;96:244–251. doi: 10.1161/01.RES.0000153979.71859.e7
 26. Hasgall PA, Di Gennaro F, Baumgartner C, Neufeld E, Lloyd B, Gosselin MC, Payne D, Klingensböck A, Kuster N. Database for thermal and electromagnetic parameters of biological tissues. *IT'IS.* 2022. doi:10.13099/VIP21000-04-1.
 27. Beitel-White N, Lorenzo MF, Zhao Y, Brock RM, Coutermarsh-Ott S, Allen IC, Manuchehrabadi N, Davalos RV. Multi-tissue analysis on the impact of electroporation on electrical and thermal properties. *IEEE Trans Biomed Eng.* 2021;68:771–782. doi: 10.1109/TBME.2020.3013572
 28. Corović S, Zupanic A, Kranjc S, Al Sakere B, Leroy-Willig A, Mir LM, Miklavcic. The influence of skeletal muscle anisotropy on electroporation: in vivo study and numerical modeling. *Med Biol Eng Comput.* 2010;48:637–648. doi: 10.1007/s11517-010-0614-1
 29. Duck FA. *Physical Properties of Tissue: A Comprehensive Reference Book.* Academic Press; 1990.